On the Significance of the Upcoming Large Hadron Collider Proton-Proton Cross Section Data

Eliahu Comay

Charactell Ltd., PO Box 39019, Tel-Aviv, 61390, Israel. E-mail: elicomay@post.tau.ac.il

The relevance of the Regular Charge-Monopole Theory to the proton structure is described. The discussion relies on classical electrodynamics and its associated quantum mechanics. Few experimental data are used as a clue to the specific structure of baryons. This basis provides an explanation for the shape of the graph of the pre-LHC proton-proton cross section data. These data also enable a description of the significance of the expected LHC cross section measurements which will be known soon. Problematic QCD issues are pointed out.

1 Introduction

Scattering experiments are used as a primary tool for investigating the structure of physical objects. These experiments can be divided into several classes, depending on the kind of colliding particles. The energy involved in scattering experiments has increased dramatically during the previous century since the celebrated Rutherford experiment was carried out (1909). Now, the meaningful value of scattering energy is the quantity measured in the rest frame of the projectile-target center of energy. Therefore, devices that use colliding beams enable measurements of very high energy processes. The new Large Hadron Collider (LHC) facility at CERN, which is designed to produce 14 TeV proton-proton (pp) collisions, will make a great leap forward.

This work examines the presently available pp elastic and total cross section data (denoted by ECS and TCS, respectively) and discusses the meaning of two possible alternatives for the LHC pp ECS values which will be known soon. The discussion relies on the Regular Charge-Monopole Theory (RCMT) [1,2] and on its relevance to strong interactions [3,4].

Section 2 contains a continuation of the discussion presented in [4]. It explains the meaning of two possible LHC results of the pp ECS. Inherent QCD difficulties to provide an explanation for the data are discussed in section 3. The last section contains concluding remarks.

2 The proton-proton elastic cross section

The discussion carried out below is a continuation of [4]. Here it aims to examine possible LHC's ECS results and their implications for the proton structure. Thus, for the reader's convenience, the relevant points of [4] are presented briefly in the following lines.

RCMT is the theoretical basis of the discussion and strong interactions are regarded as interactions between magnetic monopoles which obey the laws derived from RCMT. Two important results of RCMT are described here:

1. Charges do not interact with bound fields of monopoles and monopoles do not interact with bound fields of charges. Charges interact with all fields of charges and
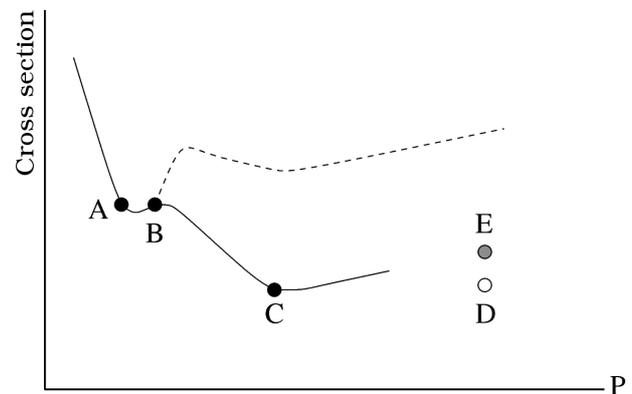
Fig. 1: A qualitative description of the pre-LHC proton-proton cross section versus the laboratory momentum P. Axes are drawn in a logarithmic scale. The solid line denotes elastic cross section and the broken line denotes total cross section. (The accurate figure can be found in [5]). Points A-E help the discussion (see text).

with radiation fields emitted from monopoles. Analogously, monopoles interact with all fields of monopoles and with radiation fields emitted from charges.

2. The unit of the elementary magnetic charge g is a free parameter. However, hadronic data indicate that this unit is much larger than that of the electric charge: $g^2 \gg e^2 \simeq 1/137$. (Probably $g^2 \simeq 1$.)

The application of RCMT to strong interactions regards quarks as spin-1/2 Dirac particles that carry a unit of magnetic monopole. A proton has three valence quarks *and* a core that carries three monopole units of the opposite sign. Thus, a proton is a magnetic monopole analogue of a nonionized atom. By virtue of the first RCMT result, one understands why electrons (namely, pure charges) do not participate in strong interactions whereas photons do that [6]. Referring to the pre-LHC data, it is shown in [4] that, beside the three valence quarks, a proton has a core that contains inner closed shells of quarks.

Applying the correspondence between a nonionized atom and a proton, one infers the validity of screening effects and of an analogue of the Franck-Hertz effect that takes place for the

proton's quarks. Thus, quarks of closed shells of the proton's core behave like inert objects for cases where the projectile's energy is smaller than the appropriate threshold.

The pre-LHC pp scattering data is depicted in Fig. 1. Let ep denote both electron-proton and positron-proton interaction. Comparing the ep scattering data with those of pp, one finds a dramatic difference between both the ECS and the TCS characteristics of these experiments. Thus, the deep inelastic and the Rosenbluth ep formulas respectively show that TCS *decreases* together with an increase of the collision energy and that at the high energy region, ECS decreases even faster and takes a negligible part of the entire TCS events (see [7], p. 266). The pp data of Fig. 1 show a completely different picture. Indeed, for high energy, both the TCS and the ECS pp graphs *go up* with collision energy and ECS takes about 15% of the total events.

The last property proves that a proton contains a quite solid component that can take the heavy blow of a high energy pp collision and leave each of the two colliding protons intact. Valence quarks certainly cannot do this, because in the case of a high energy ep scattering, an electron collides with a valence quark. Now, in this case, deep inelastic scattering dominates and elastic events are very rare. The fact that the quite solid component is undetected in an ep scattering experiment, proves that it is a spinless electrically neutral component. This outcome provides a very strong support for the RCMT interpretation of hadrons, where baryons have a core [3,4].

The foregoing points enable one to interpret the shape of the pp ECS graph of Fig. 1. Thus, for energies smaller than that of point A of the figure, the wave length is long and effects of large distance between the colliding protons dominate the process. Here the ordinary Coulomb potential, $1/r$, holds and the associated $1/p^2$ decrease of the graph is in accordance with the Rutherford and Mott formulas (see [7], p. 192)

$$\left(\frac{d\sigma}{d\Omega}\right)_{\text{Mott}} = \frac{\alpha^2 \cos^2\left(\frac{\theta}{2}\right)}{4p^2 \sin^4\left(\frac{\theta}{2}\right)\left[1 + \frac{2p}{M}\sin^2\left(\frac{\theta}{2}\right)\right]}. \quad (1)$$

At the region of points A-B, the rapidly varying nuclear force makes the undulating shape of the graph. Results of screening effects of the valence quarks are seen for momentum values belonging to the region of points B-C. Indeed, a correspondence holds for electrons in an atom and quarks (that carry a monopole unit) in a proton. Hence, for a core-core interaction, the screening associated with the valence quarks weakens as the distance from the proton's center becomes smaller. It means that the strength of the core's monopole potential arises faster than the Coulomb $1/r$ formula. For this reason, the decreasing slope of the graph between points B-C is smaller than that which is seen on the left hand side of point A.

The ECS graph stops decreasing and begins to increase on the right hand side of point C. This change of the graph's slope indicates that for this energy a new effect shows up. Indeed, assume that the proton consists of just valence quarks and an elementary pointlike core which is charged with three monopole units of the opposite sign. Then, as the energy increases and the wave length decreases, the contribution of the inner proton region becomes more significant. Now, at inner regions, the valence quarks' screening effect fades away and the potential tends to the Coulomb formula $1/r$. Hence, in this case, the steepness of the decreasing graph between points B-C *should increase* near point C and tend to the Coulomb-like steepness of the graph on the left hand side of point A. The data negate this expectation. Thus, the increase of the graph on the right hand side of point C indicates the existence of inner closed shells of quarks at the proton. It is concluded that at these shells, a new screening effect becomes effective.

It is interesting to note that at the same momentum region also the TCS graph begins to increase and that on the right hand side of point C, the vertical distance between the two graphs is uniform. The logarithmic scale of the figure proves that, at this region, the ratio ECS to TCS practically does not change. The additional TCS events are related to an analogue of the Franck-Hertz effect. Here a quark of the closed shells is struck out of its shell. This effect corresponds to the ep deep inelastic process and it is likely to produce an inelastic event.

The main problem to be discussed here is *the specific structure of the proton's closed shells of quarks*. One may expect that the situation takes the simplest case and that the core's closed shells consist of just two u quarks and two d quarks that occupy an S shell. The other extreme is the case where the proton is analogous to a very heavy atom and the proton's core contains many closed shells of quarks. Thus, the energy of the higher group of the core's shells takes quite similar value and their radial wave functions partially overlap. (Below, finding the actual structure of the proton's core is called Problem A.) The presently known pp ECS data which is depicted in Fig. 1 is used for describing the relevance of the LHC future data to Problem A.

The rise of the pp ECS graph on the right hand side of point C is related to a screening effect of the proton's inner closed shells that takes a repulsive form. An additional contribution is the repulsive phenomenological force that stems from Pauli's exclusion principle which holds for quarks of the inner shells of the two colliding protons. Now, if the simplest case which is described above holds then, for higher energies, this effect should diminish and the graph is expected to stop rising and pass near the open circle of Fig. 1, which is marked by the letter D. On the other hand, if the proton's core contains several closed shells having a similar energy and a similar radial distribution, then before the screening contribution of the uppermost closed shell fades away another shell is expected to enter the dynamics. In this case, the graph is expected to continue rising up to the full LHC energy and pass near the gray circle of Fig. 1, which is marked by the letter E [8].

The foregoing discussion shows one example explaining how the LHC data will improve our understanding of the proton's structure.

3 Inherent QCD difficulties

Claims stating that QCD is unable to provide an explanation for the *pp* cross section data have been published in the last decade [9]. Few specific reasons justifying these claims are listed below. The examples rely on QCD's main property where baryons consist of three valence quarks, gluons and possible pairs of quark-antiquark:

- Deep inelastic *ep* scattering proves that for a very high energy, elastic events are very rare (see [7], p. 266). It means that an inelastic event is found for nearly every case where a quark is struck violently by an electron. On the other hand, Fig. 1 proves that for high energy, elastic *pp* events take about 15% of the total events. Therefore, one wonders what is the proton's component that takes the heavy blow of a high energy *pp* collision and is able to leave the two colliding protons intact? Moreover, why this component is not observed in the corresponding *ep* scattering?

- A QCD property called Asymptotic Freedom (see [10], p. 397) states that the interaction strength tends to zero at a very small vicinity of a QCD particle. Thus, at this region, a QCD interaction is certainly much weaker than the corresponding Coulomb-like interaction. Now, the general expression for the elastic scattering amplitude is (see [7], p. 186)

$$M_{if} = \int \psi_f^* V \psi_i \, d^3 x, \qquad (2)$$

where *V* represents the interaction. Evidently, for very high energy, the contribution of a very short distance between the colliding particles dominates the process. Therefore, if asymptotic freedom holds then the *pp* ECS line is expected to show a *steeper decrease* than that of the Coulomb interaction, which is seen on the left hand side of point A of Fig. 1. The data of Fig. 1 proves that for an energy which is greater than that of point C of Fig. 1, the *pp* ECS line *increases*. Hence, the data completely contradict this QCD property.

- A general argument. At point C of Fig. 1, the ECS graph changes its inclination. Here it stops decreasing and begins to increase. This effect proves that for this energy value, *something new shows up in the proton.* Now, QCD states that quarks and gluons are elementary particles that move quite freely inside the proton's volume. Therefore, one wonders how can QCD explain why a new effect shows up for this energy?

Each of these specific points illustrates the general statement of [9], concerning QCD's failure to describe the high energy *pp* cross section data.

4 Concluding remarks

The following lines describe the logical structure of this work and thereby help the reader to evaluate its significance.

A construction of a physical theory must assume the validity of some properties of the physical world. For example, one can hardly imagine how can a person construct the Minkowski space with *three* spatial dimensions, if he is not allowed to use experimental data. Referring to the validity of a physical theory, it is well known that unlike a mathematical theory which is evaluated just by pure logics, a physical theory must also be consistent with well established experimental data that belong to its domain of validity. The Occam's razor principle examines another aspect of a theory and prefers a theory that relies on a minimal number of assumptions. Thus, the Occam's razor can be regarded as a "soft" acceptability criterion for a theory.

Following these principles, the assumptions used for the construction of RCMT and of its application to strong interactions are described below. The first point has a theoretical character and the rest rely on experimental results that serve as a clue for understanding the specific structure of baryons:

- A classical regular charge-monopole theory is built on the basis of duality relations which hold between ordinary Maxwellian theory of charges together with their fields and a monopole system together with its associated fields [2]. (In [1], it is also required that the theory be derived from a regular Lagrangian density.) Like ordinary electrodynamics, this theory is derived from the variational principle where regular expressions are used. Therefore, the route to quantum mechanics is straightforward.

- In RCMT, the value of the elementary monopole unit *g* is a free parameter. Like the case of the electric charge, it is assumed that *g* is quantized. It is also assumed that its elementary value $g^2 \gg e^2 \simeq 1/137$. (Probably, $g^2 \simeq 1$.).

- It is assumed that strong interactions are interactions between monopoles. The following points describe the specific systems that carry monopoles.

- It is assumed that quarks are spin 1/2 Dirac particles that carry a unit of magnetic monopole. (As a matter of fact, it can be *proved* that an elementary massive quantum mechanical particle is a spin-1/2 Dirac particle [11].)

- It is assumed that baryons contain *three* valence quarks. It follows that baryons must have a core that carries three monopole units of the opposite sign.

- It is assumed that the baryonic core contains closed shells of quarks.

The discussion carried out in [4] and in section 2 of this work explains how RCMT can be used for providing a qualitative interpretation of the shape of the graph that describes

the elastic *pp* scattering data. In particular, an explanation is provided for the relation between the pre-LHC *pp* elastic cross section data and the existence of closed shells of quarks at the baryonic core. It is also explained how the upcoming LHC data will enrich our understanding of the structure of baryonic closed shells of quarks by providing information on whether there are just two active closed shells of *u* and *d* quarks or there are many shells having a quite similar energy value and radial distribution.

QCD's inherent difficulties to provide an explanation for the high energy pre-LHC *pp* scattering data are discussed in the third section. Screening effects of proton's quarks are used in the Regular Charge-monopole Theory's interpretation of the elastic cross section *pp* scattering. It is interesting to note that this kind of screening also provides an automatic explanation for the first EMC effect [12]. This effect compares the quarks' Fermi motion in deuteron and iron (as well as other heavy nuclei). The data show that the Fermi motion is smaller in hevier nuclei. This experimental data and the Heisenberg uncertainty relations prove that the quarks' self-volume increases in heavier nuclei. In spite of the quite long time elapsed, QCD supporters have not yet provided an adequate explanation for the first EMC effect [13].

References

1. Comay E. Axiomatic deduction of equations of motion in Classical Electrodynamics. *Nuovo Cimento B*, 1984, v. 80, 159–168.

2. Comay E. Charges, monopoles and duality relations. *Nuovo Cimento B*, 1995, v. 110, 1347–1356.

3. Comay E. A regular theory of magnetic monopoles and its implications. In: *Has the Last Word Been Said on Classical Electrodynamics?* ed. A. Chubykalo, V. Onochin, A. Espinoza and R. Smirnov-Rueda. Rinton Press, Paramus, NJ, 2004.

4. Comay E. Remarks on the proton structure. *Apeiron*, 2009, v. 16, 1–21.

5. Amsler C. et al. (Particle Data Group) Review of particle properties. *Phys. Lett. B*, 2008, v. 667, 1–1340. (See p. 364).

6. Bauer T. H., Spital R. D., Yennie D. R. and Pipkin F. M. The hadronic properties of the photon in high-energy interactions. *Rev. Mod. Phys.*, 1978, v. 50, 261–436.

7. Perkins D. H. Introduction to high energy physics. Addison-Wesley, Menlo Park, CA, 1987.

8. This possibility has been overlooked in [4].

9. Arkhipov A. A. On global structure of hadronic total cross-sections. arXiv: hep-ph/9911533.

10. Frauenfelder H. and Henley E. M. Subatomic physics. Prentice Hall, Englewood Cliffs, 1991. (see pp. 296–304.)

11. Comay E. Physical consequences of mathematical principles. *Progress in Physics*, 2009, v. 4, 91–98.

12. Arrington J. et al. New measurements of the EMC effect in few-body nuclei. *J. Phys. Conference Series,* 2007, v. 69, 012024, 1–9.

———————————